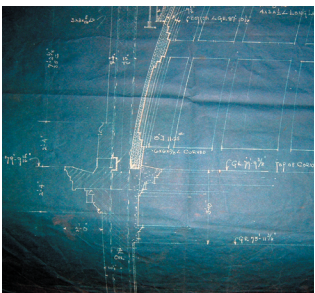
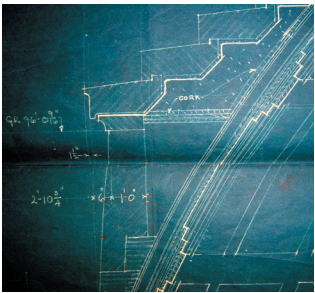
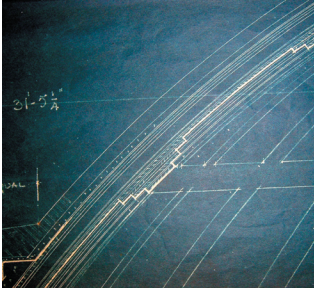


# The First Church of Christ, Scientist Cambridge, Massachusetts

A Historical and Structural Study of the Main Dome



Wanda W. Lau  
4.448 Analysis of Historic Structures  
Professor J. A. Ochsendorf  
13 December 2004

## Table of Contents

<i>Introduction</i> .....	1
Background .....	1
Objectives .....	1
Resources .....	2
<i>Part One: The History</i> .....	3
The Need for a Church.....	3
Selecting a Designer .....	4
The Guastavino Fireproof Construction Company.....	4
Overview of The First Church of Christ, Scientist, Cambridge .....	5
Construction Features and Methods .....	6
<i>Part Two: The Structure</i> .....	9
Domes .....	9
The Membrane Theory.....	10
Limit State Analysis of Masonry .....	10
Parameter Definitions.....	11
Dome Geometry and Assumptions .....	12
Methodologies.....	13
Results .....	17
Tension Ring.....	18
Compression Ring.....	19
Limit States .....	19
<i>Summary</i> .....	21
State of the Art .....	21
The First Church of Christ, Scientist, Dome.....	21
The End of an Era.....	21
Future Work .....	22
<i>Figures</i> .....	23
<i>Tables</i> .....	32
<i>References</i> .....	34
<i>Appendices</i> .....	36

## **Introduction**

This report examines the construction history, structural behavior, and design intention of the main auditorium dome of the First Church of Christ, Scientist, located on 13 Waterhouse Street, Cambridge, Massachusetts. In addition to the dome, the church contains a number of works by The Guastavino Company, whose cohesive construction technology remains aesthetically and structurally remarkable in building designs to date.

## ***Background***

Existing publications on The Guastavino Company typically provide an overview on the history, development, and innovations of the Company with limited detailed descriptions on some well known projects, such as the Boston Public Library and St. John the Divine Cathedral. Rarely do the publications discuss the methods of structural analysis employed by Guastavino, perhaps because little is known aside from what Guastavino revealed in his few publications and from what may be gleaned from the Guastavino archives in Avery Library, Columbia University. From the few publications that do exist, even fewer discuss the theories on which Guastavino based his design methodologies, and none elaborate on specific Guastavino dome projects.

Though the First Church of Christ, Scientist, in Cambridge is an outstanding example of Guastavino construction, it remains unstudied and relatively obscure compared to other Guastavino projects. Current texts do little more than acknowledge the Church by name in a long list of Guastavino's projects. The Cambridge Historical Commission describes the Church as bringing "monumental emphasis and spatial definition" to its prominent location, but provides scarce additional detail while failing to reference Guastavino in the design (Cambridge, 1973). In summary, to quote one of church members encountered in the research phase of this project, "No one has ever studied our Church before."

## ***Objectives***

The overall objectives of this study may be summarized in the following manner:

1. Provide a historical account and setting for the construction of the Church dome.
2. Perform a simplified structural analysis of the main dome.

However, as will be seen, the nature of this topic inherently weaves the two objectives together, thus blurring any line that attempts to distinguish them.

## **Resources**

This study consulted numerous resources to provide an accurate account of the Church construction, historical context, and geometry and components of its main dome. The following are some primary resources used in this study (comprehensive list in References):

1. *History of the First Church of Christ, Scientist, Cambridge, MA 1899 – 1996*
2. Original architectural drawings by Bigelow and Wadsworth (revised 1929)
3. Original structural drawings by Charles L. Shedd (1923 - ?)
4. Original dome section drawing, Drawing No. 9, by R. Guastavino Co. (1929)
5. Correspondence between R. Guastavino Co. and Bigelow and Wadsworth (1920 – 1931)
6. Archived documents from the Guastavino archive in Avery Library, Columbia University.

In addition, a number of texts on the membrane theory of analysis for domes served as references for the graphical and analytical structural analyses.

## **Part One: The History**

To appreciate fully the historical significance of the Church, this study discusses not only the Church construction and design processes, but also the backgrounds of its designers and some unique features of the main dome.

### ***The Need for a Church***

As legend goes, on 3 January 1899, Mary Baker Eddy, founder of Christian Science and the Mother Church in Boston, Massachusetts, summoned the formation a branch church across the Charles River in Cambridge (First Church, 1996). Within months, church members established the First Church of Christ, Scientist, at the first of several locations in Harvard Square, finally settling on the Church's current site at 13 Waterhouse Street in December 1917. Due to increasing membership, the Church building committee decided to construct a new building, selecting the Boston-based firm of Bigelow and Wadsworth<sup>1</sup> as their architect. Giles M. Smith, a church member and architect at the firm, was designated to lead building operations.

Church members found design inspiration in the Roman Pantheon and Thomas Jefferson's University of Virginia Library (now Rotunda), and in particular, the absence of obstructing columns in the circular auditorium of the Pantheon. In the autumn of 1919, Bigelow and Wadsworth submitted a proposal based on these landmarks to unanimous approval from church members.

To prevent excessive debt, members divided the construction into two phases, the first of which commenced in January 1924 (Appendix B.1.a). The first phase included a large basement-level room with a flat dome ceiling up to one level above ground to a belt course (Figure 1). Five years later, the second phase commenced when a financial plan was secured between the Church and Joseph Willcutt, a congregation member and building contractor who would later work on the church construction. The second phase included the upper four floors of the Church in addition to its showcase piece, the main dome of the auditorium, in where the celebratory first services were held on 30 April 1930 (Figures 2 and 3, Appendix B.1.d).

---

<sup>1</sup> In 1928, the architecture firm of Bigelow and Wadsworth was renamed Bigelow, Wadsworth, Hubbard and Smith prior to the commencement of the second phase of construction of the Church. The firm underwent several iterations of names before Giles M. Smith and Philip Wadsworth finally ended their formal careers as independent architects in 1942 (MA COPAR, 1984).

### ***Selecting a Designer***

With the University of Virginia Rotunda as a model for the Church design, Bigelow and Wadsworth needed a designer for the vaults and main dome. Their thoughts may have flashed back first to the Worcester County Institution of Savings, Worcester, MA, where Henry Bigelow had collaborated with a masonry designer and architect on the large low-rise dome in 1905 to 1906 (Huerta, 1999). This masonry designer had also designed the dome in the Mother Church in Boston and equally appropriately, the 1898 reconstruction of the grand dome of the U-VA Rotunda itself. For the design of the future dome of the Church, Bigelow and Wadsworth selected The Guastavino Fireproof Construction Company.

### ***The Guastavino Fireproof Construction Company***

#### *Overview*

Rafael Guastavino i Moreno was an established architect and builder in Barcelona, Spain, by 1873 (Parks, 1996). Trained in the art of Catalan construction and timber vaulting, Guastavino immigrated to the United States in 1881, bringing with him to New York his innovative construction methods, which he would later term “cohesive construction,” and his nine-year old son, also named Rafael, who would soon follow in his father’s footsteps (Parks, 1996). After a few small projects, Guastavino focused on marketing the fireproof abilities of his construction methods and founded the Guastavino Fireproof Construction Company in 1889. For the next 70 years, the Guastavino company would contribute to the design of over 1,000 known projects in the U.S., and hold twenty-four patents in a wide range of areas in construction, several of which are used in the Church.

#### *Cohesive Construction*

Cohesive construction involves setting lightweight terra cotta tile masonry in rapid set hydraulic cement to construct very thin, rigid, and strong structural surfaces such as timber vaults and domes (Tarragó, 2002). The surfaces have a thickness of often no more than 2 tiles (about 3 in.) and can support large loads due to their geometries (Figure 4). The mortar between tiles acts similarly to plaster-of-Paris, achieving a near instant bond and set. Analogous to plywood and its binder, the tiles and mortar act monolithically; the tiles will typically split apart before the mortar bond between tiles fails (Tarragó, 2002). Subsequently, cohesive construction can support load almost immediately and often does not require centering or formwork during construction. The non-combustible properties of the terra cotta and cement elements provided

Guastavino the marketing opportunity needed to impetus the Guastavino Company into the building design industry in America.

### *The Designer*

In the spring or summer of 1920, Bigelow and Wadsworth contacted R. Guastavino Company to participate in the structural design of the Church (Appendix B.2.a). Guastavino, Sr., had lost the battle to lung disease twelve years earlier and his son had transitioned seamlessly to leading the company. Guastavino, Jr. began working with his father at the age of 15 and had participated in the design and construction of a number of notable timbrel vaults, including domes, with his father before his death (Figure 5).

In addition to learning from his father's methods of cohesive construction, Guastavino, Jr., also researched graphical methods of structural analysis in vault and dome design in order to estimate tension stresses and size iron reinforcement (Huerta, 2003). In 1910, his understanding of dome behavior culminated into a patent for incorporating reinforcement in cohesive construction of masonry vaults (Appendix B.3). In the years leading up to the Church commission, Guastavino, Jr., had designed a number of domes in religious and commercial institutions, including the stately domes at the Tenth Church of Christ, Chicago (1917) and the University of Pennsylvania Museum (1912).

From this point forward, references to Guastavino in this study are in reference to Guastavino, Jr., unless noted otherwise.

### ***Overview of The First Church of Christ, Scientist, Cambridge***

Situated on the edge of Cambridge Common, the Church stands 40 ft above grade, extends upward an additional 40 ft to the skylight crowning the main dome, and extends downward two floors below grade for the basement and sub-basement (Appendix A.1.b). In addition to the main dome, the Church contains a number of Guastavino designs: the masonry brick barrel vaulting at the sub-basement level, the shallow timbrel dome at the basement level with a span comparable to that of the main dome, and the timbrel vault in the main lobby with the signature herringbone tile pattern. Inside the auditorium, a barrel vault over the gallery intersects the main dome; this vault acts as a hung ceiling rather than an additional means of support for the dome (Appendix B.2.c).

### *The Main Dome*

The main dome interior is finished with glazed blue-gray tile coffers with an oculus or opening at its crown (Figure 6). A skylight at the oculus allows natural light into the auditorium although in the original Church design, a large translucent glass suspended from the oculus edge covered the skylight, diffusing light entering into the space below. The skylight consists of a terra cotta base and metal framed glazing.

The dome exterior is clad with limestone, which was subsequently covered with lead-copper flashing due to leakage in 1933, three years after the dome's completion. Figure 7 shows a typical section through the main dome. Large limestone cornices encircle the dome base. The dome sits on the continuous cylindrical wall of the auditorium with the exception of the gallery at the barrel vault intersection (Appendix A.1.b).

### *Structural Steel*

Steel framework inside the cylinder wall supports the combined weight of the dome, overburden and surcharge (Appendix A.1.d). Near the base of the dome, an iron curved girder transfers the load of the dome and surcharge above this point to the main girder 'A' (Figure 8). Unlike the curved girder which is 'continuous' around the cylinder wall, Girder 'A' members form a 16-sided polygon in plan view. Girder 'A' members are connected to steel columns that carry the load down the height of the building to the foundation at the sub-basement level. A solid brick infill fills the void under the girders outboard of the bottom coffer band around the main dome.

### ***Construction Features and Methods***

The main dome of the Church features several trademarks of Guastavino design and construction, some of which are described below (Appendix A.2).

### *Tension Components*

Like his father, Guastavino was aware of the necessity of providing resistance to outward thrust generated in the flow of forces due to dome geometry. Tile masonry has low, if any tensile strength, and for the dome structure to maintain a constant radius and thickness the full height of the dome, Guastavino employed a number of methods to contain the line of thrust or applied force line within the structure that are typical in many of his domes, such as the National Museum of Washington, D.C., (1906) and St. John Cathedral, New York City (1908) (Huerta, 2003).

At an angle of 55° from the central axis, a steel tension angle is embedded into the flat tile work of a dwarf vault that rests on 4 in. thick walls every 4 ft on center. At an angle of 72° the largest tension member, a ring comprised of a plate and two angles, is installed. A final angle is installed at the bottom edge of the dome at an angle of 89°. The tension steel components are curved in plan, suggesting Guastavino was aware of the vulnerabilities at discontinuous joints or the 'corners' of the polygon framing where splices are not easily achieved for a tension ring. In addition, Guastavino used the weight of the solid masonry infill, increased tile thickness, and massive exterior cornices at the dome base to provide additional tension resistance.

### *Tile Masonry*

The blue-gray finishing tiles of the dome coffers are another patent of Guastavino who collaborated with a Harvard physicist named Wallace Clement Sabine for this invention. Akoustolith cast stone tile, marketed for its sound absorbing and incombustible fire resistance qualities, consisted of well-graded aggregate and a Portland cement based binder (Pounds, 1999). Naturally colored white or gray, the tile attained a variety of hues depending on the aggregate type used in the production process and the temperature at which the kiln was fired (Figure 9, Appendix B.4.a). For example, the shade of the dome tiles suggests the use of slate aggregate in its composition. Akoustolith tiles came in a variety of sizes; for the Church dome coffers, 6 in. by 12 in. tiles are used in the outboard course of the ribs or raised bands of the coffers as well as in the herringbone face tile of the coffer inlay, and 6 in. by 6 in. tile in the 'steps' of the ribs. Each tile is 1 in. thick and weighs 4 pounds per square foot; including mortar, three tile layers have a combined thickness of 4 in. (Appendix B.4.a). Based on laboratory tests conducted in 1927 and 1935 at the Massachusetts Institute of Technology, each Akoustolith tile has a compressive strength of about 1,000 pounds per square inch (psi) (Appendix B.4.b).

In addition to the Akoustolith finish tile, two courses of 15 in. structural 'rough' tile fill the space between coffers, unifying the monolithic dome structure; these tiles may be Akoustolith, but rough unfinished tile was likely used for both structural and economical reasons. These courses, hidden from the public eye, are corrugated with the direction of the ribs altering between adjacent courses (Figure 10). The corrugations increase the available surface area for the plaster cement mortar to cover, the bond between tiles, and the distribution of loads through the structure. The structural tiles have an average compressive strength between 4,000 and 9,000 psi, depending on the direction of the ribbing with the loads and the ceramic burning process (Appendix B.4.b).

Guastavino, Sr., published information on the tensile strength of the tile, but because this value was relatively low and achieved in controlled laboratory settings, this study assumes the masonry tiles have no tensile capabilities (Guastavino, 1893).

### *Coffers*

The ribs of the coffers consist of tiles stacked three high in the longitudinal and latitudinal directions. Thirty-two longitudinal ribs divide the dome into 32 slices; eight horizontal bands divide the slices into seven equal arcs.

Although one distinguishing feature of cohesive construction was its ability to be constructed without the use of centering or scaffolding, centering was used for the Church dome construction because of the coffer finish (Appendix B.2.c). Workers first assembled the coffers as prefabricated individual units, and then used the wood centering, which traced the curvature of the dome, as supports against which to lay the coffers (Figure 11). On the outboard side of the dome, workers filled the voids between the recesses of the coffers with structural rough tile and cement mortar. Although the exact composition of the prefabricated units is not known, it is probable that the units contained the finish Akoustolith tile set in plaster in their designated herringbone patterns and ribs due to the perfect geometry of the tiles as seen inside the Church auditorium. Alternatively, the units may have served as molds into which workers placed the tile and plaster cement directly while supporting themselves and the molds with the scaffolding.

## **Part Two: The Structure**

The following simplified structural analysis of the main dome was performed for several reasons:

1. To understand Guastavino's intention in the design of the main dome, and the extent of structural knowledge illustrated through his design.
2. To compare results attained from the analytical and graphical approaches of the structural analysis, both of which are based on the simplified membrane theory for domes.
3. To determine the safety and limit states of the dome as built.
4. To explore the effects of hypothetical design configurations on the structural behavior of the dome.

### ***Domes***

Simply put, a dome is a curve revolved about a central axis to form a surface that serves primarily as a roof structure. The curve may assume an infinite number of geometries; for the Church, the curve is circular and maintains a constant radius. In terms of structure, a dome must satisfy three criteria: strength, stiffness, and stability. The dome must be capable of supporting applied loads including its self weight without excessive deflection and without unstable displacements (Heyman, 1996).

Similar to an arch, the applied forces or loads travel down a dome's meridians to its base and are resisted by a support structure. The line of thrust, or the path on which the forces travel, is the ideal shape of an arch that supports these loads (Heyman 1995). Unlike an arch, a dome can resist potential out-of-plane bending of the meridians with its hoop forces, which act in the latitudinal direction of the dome as parallel stiff rings (Figure 12) (Billington, 1982).

At the base of a dome, the support structure must resist the inclined forces with equal and opposite reactions (Figure 13). The vertical component of the inclined force, or gravity load, is typically resisted with ease by the support structure; for the Church, the steel framework within cylindrical wall of the auditorium comprises this structure. The horizontal component or thrust must also be resisted, particularly at the base of the dome. Several methods exist to supply this horizontal resistance, such as massive support structure walls that buttress against the thrust as in the case of the Pantheon and its 20 ft thick walls, or a separate support structure, such as a metal tension ring along the circumference (Heyman, 1995). Thus at its base, the dome may have a continuous fixed support to the walls below; that is, it has the potential to transfer

moment resulting from the horizontal thrust into the support structure below. However, it is typically more desirable to assume that the dome is simply supported; that is, the design does not transfer the thrust into its support structure. Subsequently only vertical loads are transferred to the support structure.

### ***The Membrane Theory***

The membrane theory is the basis of the current methodology of dome structural analysis and provides a reasonable approximation for thin-shelled domes (Heyman, 1996). A dome shell may be considered thin when its thickness is less than 5 percent of its local radius of curvature, or its  $t/R$  ratio is less than 0.05 (Heyman, 1996). Based on the assumed thickness for the Church dome of 3 in., the  $t/R$  ratio equals 0.008. The membrane theory assumes the following (Figure 14) (Heyman, 1995):

1. Applied loads are resisted by internal forces within the surface, which has no stiffness against bending; therefore internal forces are either pure tension or pure compression.
2. On a symmetrically and uniformly loaded dome, internal forces act perpendicular to each other in the meridional and latitudinal hoop directions.
3. Internal forces are coplanar; that is, the membrane has zero thickness.
4. The membrane plane is located along the centerline of the actual dome thickness; thus the lines of thrust must also follow the centerline.

The last assumption, which constrains the line of thrust to a two-dimensional plane along the centerline of the dome, merits discussion. In reality, many lines of thrust may lie within the finite thickness of the dome, all viable solutions for a stable structure. Furthermore, the lines of thrusts in the meridional and hoop directions may not coincide. The thickness of the structure only defines a permissible region within which a membrane solution must be found (Heyman, 1996). Therefore the membrane theory operates on the lower bound principle: if one solution is found by assuming the line of thrust at the centerline that achieves stability and equilibrium, then the structure will also find its own solution.

### ***Limit State Analysis of Masonry***

Because the Church dome is a masonry structure, the limit state analysis of masonry applies, which assumes the following (Heyman, 1995):

1. Masonry, particularly the mortar joints in masonry, has no tensile strength.
2. Compressive stress levels from loads applied to the structure are low relatively to the crushing stress of masonry; thus material strength properties are not of concern.

3. Sliding failure does not occur.

Each assumption has its limitations. For example, Guastavino, Sr., observed that the mortar or plaster joints have greater tensile strength than the tiles themselves in his cohesive construction. To be conservative, this analysis will assume the limit state applies.

### ***Parameter Definitions***

In the structural analysis of the dome, polar coordinates (radius, theta  $\theta$ , phi  $\Phi$ ) locate a point along the dome surface in reference to the center of the dome (Figure 15). For the Church dome, whose surface consists of a complete revolution about the vertical axis,  $\theta$  equals 360 degrees. Phi is measured in the meridional direction from the vertical axis with  $\Phi = 0$  at the dome crown. Half of the angle of embrace, the amount of a sphere contained in the dome, is assigned a unique  $\Phi$ -value of  $\alpha$ .

As discussed earlier, internal forces in the dome may act in the meridional or hoop direction (Figure 16). These forces are calculated as stress resultants in the unit of force per length. Meridional stress resultants,  $N'_\phi$ , transfer the vertical gravity loads to the dome base, bringing with them a horizontal component or thrust,  $H$ , that propagates into the inclined reaction at the base (Figure 13). Meridional forces are in compression and increase from the crown to the base of the dome as the gravity load accumulates.

Near the crown of the dome, the hoop stress resultants,  $N'_\theta$ , are in compression; the masonry is pushing against its neighbors to resist collapse inward. Toward the base of the dome, the hoop forces transition to tension; the masonry is holding onto its neighbors to prevent the base of the dome from splaying into its desired shape, that of a catenary line. For a dome with uniform loading, this transition occurs at  $\Phi = 51.8$  degrees (Heyman, 1995). The dome must provide tension resistance to prevent bursting; for masonry structures such as the Church dome, an alternative means must be provided.

Because this analysis assumes the applied loads on the Church dome are axisymmetrical, forces do not change as one progresses around the dome in the hoop direction, unlike the forces which progressively change from crown to base in the meridional direction (Billington, 1982). Therefore, this analysis assumes negligible shear forces,  $N'_{\phi\theta}$ .

### ***Dome Geometry and Assumptions***

In general, geometry is the primary factor in determining the structural behavior of a dome. The main dome of the Church auditorium spans approximately 65 ft with a rise of 30 ft from the dome base. This analysis assumes that the dome is simply supported on the vertical cylinder wall of the auditorium; that is, continuous support to the dome is only provided in the vertical direction with no transfer of bending forces. The radius of the dome,  $a$ , is measured between the center of the dome and the membrane plane, which was assumed between the two complete courses of the structural tile (Figure 7). The angle of embrace of the dome is approximately 170 degrees, half of which is assigned the  $\Phi$ -value,  $\alpha$ . Additional noted  $\Phi$ -values correspond to the location of the skylight edge and the installed metal tension rings.

For a conservative analysis, the dome structure has a thickness of two structural tiles plus its shared mortar joints, or 3 in. In addition, though Dwg. 9 shows an optional tensile rod at  $\Phi = 66$  deg., the analysis will assume it was not installed (Appendix A.2). The skylight is assumed incapable of carrying loads. Reinforcement in the meridional direction is not shown on the dome drawings; this analysis assumes likewise. Figure 17 summarizes the dome geometry and parameters this analysis assumes.

The meridional tile ribs of the coffers define the 32 slices or lunes into which the dome was divided for this analysis (Figure 18). Similarly, the latitudinal tile ribs divide each lune into seven sections or what will be termed “voussoirs” hereon in. Translating the meridional and hoop stress resultants into forces and stresses requires the dimensions of each voussoir. The length of the arc in section,  $u$ , and the thickness,  $v$ , of each voussoir are constant due to the coffer definitions (Figure 19). For each voussoir,  $w$  is the average width of each voussoir between consecutive latitudinal coffer ribs, and increases with angle  $\Phi$  (Figures 20 and 21). This analysis uses the dimensions to determine the magnitude of applied loads, and to convert stress resultants from the analytical approach of the membrane theory.

### ***Applied Loads***

The dome must support dead loads or its self weight, and live loads, which include snow, rain, and wind. This analysis divides the self weight of the dome into three categories: uniform dead load consisting of the total weight of materials shown in a typical section through the dome thickness (Figure 7); concentrated load at the oculus due to the skylight and light fixtures; and a axisymmetrical surcharge load due to the cornices and solid brick wall infill at the dome base.

The *1924 City of Cambridge Zoning Law and Building Code* gives values for vertical snow and rain live loads; live loads are based on the horizontal projected area of the Church dome and, but are divided by the dome's total surface area to simplify the analysis. This analysis does not include the lateral load, wind, because of its relatively negligible influence on internal forces. The surcharge load ranges from zero pounds per square foot (psf) at the crown to about 450 psf near the base of the dome. Figure 22 shows the magnitudes and locations of the applied loads.

### ***Reactions***

From Figure 21, the support structure carries a total gravity load of 1,705 kips. This load represents the vertical component of the inclined meridional force at the base of the dome where  $\Phi = \alpha = 85.9$  degrees. The horizontal reaction or thrust of the meridional force must be resisted by tension components to constrain the line of thrust within the dome structural thickness, which for this analysis does not include the solid masonry fill at the dome base (Appendix A.2). Only vertical load is transferred to the support structure; this gravity load divided by the perimeter of the cylinder wall equals the reaction,  $V$ , or 8.28 kips per foot (Figure 23).

To obtain the horizontal reaction, the internal meridional and hoop forces must be calculated at different angles of  $\Phi$  along the arc length of the dome. The forces may be obtained by graphical or analytical methods. Both methods utilize geometry as their starting point.

### ***Methodologies***

In *Essay*, Guastavino, Sr., discusses his reasoning behind his calculation methods for the design of vaults and domes. His calculations, based partly on equilibrium and partly on his theory of cohesive construction, do not involve the elastic theory in the analysis of masonry, which was favored by engineers at the end of the 19<sup>th</sup> century (Huerta, 2003). Although his writing contains some incorrect assumptions on the geometry and behavior of domes due to inconsistencies in his cohesive theory, Guastavino, Sr., understood the behavior of a dome is based on its form and not its material. By combining his cohesive theory with his correct use of the equilibrium approach and some graphical analysis, he was able to design structures within reason and with enough safety (Huerta, 2003). His son however delved further in the use of graphical analysis in the design of domes.

### *Graphical Analysis*

Graphical analysis provides a visual method of solving for structural equilibrium through the knowledge of building geometry and forces. In 1878 Henry T. Eddy, a civil engineering professor at the University of Cincinnati, first proposed a graphical analysis method for thin shell domes based on assumptions postulated by the membrane theory, whose analytical formulae had begun evolving 20 years prior. In 1904 and 1908, Eddy's methods were resurrected and popularized in articles published by William Dunn, a British engineer (Huerta, 2003).

When Guastavino was commissioned to design the Church dome in 1922, he had much experience in vault design through graphical analysis as popularized by Dunn and some simple equilibrium formulae (Appendix B.4.c) (Huerta, 2003). Like his father, Guastavino intuitively understood the behavior of meridional and tensile forces in dome structures. In his Masonry Structure Patent (Appendix B.3.a), Guastavino demonstrated his understanding of the need for metal tensile reinforcement in specific regions of high stress, particularly the oculus and the base of a dome.

Guastavino took advantage of Eddy's observation that thrust becomes constant for unreinforced masonry domes beyond a certain angle  $\Phi$ , whose value depends on structure geometry and loading. By manipulating dome structures from perfectly spherical in its upper region to a shape tracing the catenary line of force below the region at where zero hoop force occurs, Guastavino could design domes without any tensile reinforcement except a hoop ring at the base (Huerta, 2003). The 1904 design of the double dome at the Bank of Montreal, Ontario, is an early example demonstrating this comprehension.

However Guastavino did not employ the hybrid spherical-catenary design in his design of the Church dome. Perhaps either the church or the architects specified a constant radius for the Church dome to mimic in strict accordance with the domes of the Pantheon and U-VA Rotunda. Thus, Guastavino placed a number of tension components in the dome, including solid brick infill, dwarf vaults, and metal tension members, whose locations will be examined later.

The graphical analyses performed in this study are based on methods described by William S. Wolfe in his 1921 textbook, *Graphical Analysis: A Textbook on Graphic Statics*. Information obtained from a graphical analysis includes meridional and hoop forces along the arc of a dome, horizontal thrusts, and the deviation of the thrust line from the line of the assumed membrane in

cases where no tensile capabilities of the dome structure are assumed. Results from the graphical approach are in units of force (e.g., pounds).

In addition to limitations associated with the membrane theory and limit state analysis of masonry, the graphical method has limitations. The method does not distinguish between load types; that is, distributed, variable and concentrated loads are all translated into a magnitude of vertical load, weight, though they generate internal forces differently. For example, the concentrated load at the oculus generates meridional and hoop forces at the oculus edge or compression ring; however, the graphical analysis redistributes the load to the centroid of the first voussoir, thus eliminating internal force values at this edge condition. This graphical method does not indicate whether incomplete domes, such as the Church dome with its oculus, are analyzed differently. The accuracy of the graphical analysis depends also on the resolution of how the structure is divided (i.e., number of lunes).

This study analyzed four case studies; Table 1 lists the assumed conditions for each case. The “variable” load condition indicates uniform dead and live loads ( $w_d$  and  $w_l$ ), the variable surcharge load ( $q$ ), and the concentrated load at the skylight ( $p$ ) are included in the analysis (Figure 22). The “uniform” load condition indicates only the uniform dead and live loads are factored into the analysis. For the case of “tension”, the structure is assumed to have tensile capabilities due to incorporated tension components. For the case of “no tension,” the dome is assumed to have no tensile reinforcement. The complete analyses for the four case studies are shown in Appendix C.

### *Analytical Analysis*

Though formulae for membrane analysis of domes was introduced as early as 1858, it was not until 1926 when a mathematical theory describing the behavior of dome shells of revolution became simplified enough for practical use (Huerta, 2003) (Billington, 1982). The original design of the Church preceded the publication of this theory by at least two years; therefore, it is unlikely that Guastavino utilized this approach. However, the membrane theory remains the basis of most modern engineering methods that model the behavior of domes.

The analytical method utilizes geometry and calculus to calculate the change of internal forces from one side of the element to another side of an infinitesimally small element of the dome. The sum of these forces must establish equilibrium in directions tangential to the meridians, normal to the dome surface, and parallel to the latitudes for the entire dome structure (Heyman,

1977). These forces are integrated over the arc length of a curved plane from the crown to base to find the total stress resultant, meridional or hoop, at any angle  $\Phi$ . Equations for internal stress resultants vary for different types of load application and dome geometries. For the Church, the final stress resultant at each angle  $\Phi$  equals the sum of the internal forces contributed by each load type. Table 2 summarizes the equations used in the analytical analysis (Billington, 1982). Refer to Figures 17 and 22 for the variables.

The equations give linear force values in units of force per length. To convert the linear forces into forces in units of pounds, the meridional stress resultants are multiplied by  $w$ , the average width of each voussoir in plan view, and the hoop stress resultants are multiplied by  $u$ , the arc length in section view (Figure 19). The stress resultants are both divided by the structure thickness  $v$  to obtain values in units of pounds per square inch.

The membrane theory has limitations particularly at edge conditions. For example, in plan view, the uniform linear load due to skylight produces an inwardly directed compression force at the dome edge where a compression ring is assumed. In general this force is not equal to the hoop stress calculated in the adjacent area of the dome. As a result, incompatibility occurs due to the different elastic strains, or changes in dimension, between the ring and dome structure (Heyman, 1977). Similar incompatibility occurs in regions where the tension bands intersect the dome structure in compression. Some local bending in this region will occur, which is not addressed in the basic membrane theory. In addition, the membrane theory does not account for errors due deformations such as translation and rotation, and stress and strain properties of materials. However the regions at where these errors occur are limited; in general, the membrane theory may be considered to provide a reasonable approximation of dome behavior (Heyman, 1977).

Because the analytical method does not distinguish between conditions structures with and without tensile resistance, only Case Studies 1 and 3 from the graphical analysis apply. Though masonry is assumed to have no tensile resistance, the calculated tension hoop forces combined with the horizontal thrust values provide insight into Guastavino's sizing of the metal tension bands. Appendix D contains the complete analyses for the two case studies.

## **Results**

For simplicity, only the results for Case Study 1 are used to compare the analytical and graphical approaches; Case Study 1 most closely portrays the in-situ dome conditions and provides values for comparison from dome crown to base. The remaining case studies are used to examine effects on the dome behavior by altering various parameters. Figure 24 summarizes the overall forces on the structure based on both methodologies. Figures 25 and 26 show the location at where the internal forces are calculated for each lune.

### *Meridional Forces*

Meridional forces at angles  $\Phi$ , the approximate centroid of each voussoir, from both methodologies are listed in Figure 27. Table 3 summarizes the results for both methodologies. For the analytical analysis, the sum of linear forces contributed by the different load types for each voussoir is listed in addition to the resultant force  $P_\phi$ . For the graphical analysis, the analysis assumes the average of adjacent meridional force values,  $P_\phi$ , measured on the force polygon represents the force at the common centroid; for example,  $P_\phi$  at voussoir 2 is the average of the forces at spaces B and C on the force polygon (Appendix C). Discrepancies between the methodologies are listed in terms of percentage. As predicted, the meridional forces increase in compression from the dome crown to base as the self-weight of the dome increases. At the base of the dome where  $\Phi$  equals  $\alpha$ , the meridional force is 8.3 kips/ft. The vertical component of this force is equal to  $(8.3 \text{ k/ft}) * (\sin 86^\circ) = 8.3 \text{ k/ft}$ , which equals the vertical reaction,  $V$ , calculated directly from the weight of the dome.

### *Hoop Forces*

Hoop forces at angles  $\Phi$  at each voussoir are summarized in Table 4. The sum of linear forces contributed by the different load types for each voussoir is listed in addition to the resultant force,  $P_\theta$ . For the graphical analysis, hoop force values are converted from direct measurements on the force polygon. The surcharge load at the dome base shifts the zero hoop force location between compression and tension to approximately  $67^\circ$  (Figure 28); that is, the surcharge load forces rings near the dome base into compression in the hoop direction rather than tension. Tension hoop forces shown in the figure are for comparisons between the two approaches and for examining Guastavino's rationale for placing tension. At these locations, the dome relies on alternative means of tension resistance. Hoop forces at the edge conditions, that is, the skylight collar and the dome base, are not listed; these areas are discussed below.

### *Discrepancies*

The large discrepancies in internal forces between the different methodologies occur primarily at edge conditions where the concentrated and surcharge loads are applied. Simplifications and assumptions made in each methodology contribute to the discrepancies, but two other explanations will be posed. The analytical method assumes each applied load type (e.g., uniform, variable) uniquely affects the dome behavior. However, as stated earlier, the graphical method converts all loads to a locally uniform load. In the graphical analysis, the analysis attempted to apply the skylight point load at the oculus edge, but its impact on the force polygon was negligible due to its relatively small magnitude. The effect of the load simplification of the graphical analysis is evident from Case Study 3 where both approaches consider only uniform dead and live loads, and discrepancies at edge conditions between methodologies are slightly lower (Appendix D.4). The graphical approach may also require adjustment for the incomplete dome geometry, which may have contributed to the edge discrepancies. Rather than fine tuning each approach, the analysis draws conclusions by considering the methodologies together.

### *Tension Ring*

The dome must provide resistance to the horizontal thrust of meridional forces. Theoretically, tension hoop forces compensate for the outward thrust (Figure 29); however this cannot be relied on for the Church dome. The horizontal thrust values from the analytical approach are listed in Table 5. Because these values derive from meridional force, percent discrepancies between the approaches are equal and are not shown. The highest thrust value,  $H = 1.75$  k/ft outward, occurs between voussoirs 6 and 7, where  $59^\circ < \Phi < 70^\circ$ . Subsequently the dome experiences its maximum tension force,  $T$ , in this region; the value of the force is about 53.7 kips (Appendix D.3).

Not surprisingly, it is in this region that Guastavino placed the three metal tension rings (Fig. 28). If the stone and masonry surcharges were installed simultaneously with the dome, the zero tension force where hoop forces no longer are effective occurs at  $\Phi = 69^\circ$ , exactly where the largest tension ring is placed. However, if a delay between the surcharge and dome installations occurred, the zero tension force occurs at  $\Phi = 54^\circ$ , almost exactly where the first tension component is placed (Figure 30). By designing three mandatory tension rings, Guastavino approached the design conservatively and anticipated both possible construction sequences, even adding a twisted rod at  $\Phi = 65^\circ$  if the “exterior stonework is (not) built at same time as dome” (Appendix A.2).

Based on gross steel area and assuming continuous bands around the dome, this study approximates the smallest tension band member, an equal-leg 3 in. by 3/8 in. thick angle, requires only a yield strength,  $F_y$ , 30 kips/in.<sup>2</sup> to sustain the maximum tension alone, a reasonable strength for construction steel in 1929 (AISC, 1998) (Appendix D.3). However, the metal rings work in conjunction to counteract tension forces, and are placed at these intervals to continuously adjust the line of thrust from escaping the dome thickness as needed. The surcharge of the brick infill and limestone cornices in this region also contributes to constraining the line of thrust.

Since the dome is assumed to be in equilibrium, tension forces in the metal rings must be equaled by compressive forces in the structure, which internal hoop forces provide. Therefore, the calculated total tension in the rings should equal the sum of the compression hoop forces (Appendix D.3); this sum is 51.2 kips, which is nearly equal to the tension force of 53.7 kips.

### ***Compression Ring***

The line load,  $p$ , from the skylight and light fixtures apply a concentrated vertical load on the oculus edge of the dome. Since the dome shell can only provide resistance in a direction tangential to the shell, such as meridional and hoop forces, the edge of the dome must be stiffened in compression to supply the required horizontal thrust to support the load (Billington, 1982) (Figure 31). This analysis assumes the compressive ring is monolithic or incorporated with the dome structure. The thrust creates a circumferential compression at the oculus edge of 3.8 kips. If the compressive strength of the masonry tiles is 1 kip per square inch (ksi), the most conservative value from strength properties for the Akoustolith and structural tile, and the assumed structure thickness is 3 in. or two tiles thick, then the skylight load is distributed over an internal compression ring of width 11.3 in.

### ***Limit States***

The analysis examines two limit states or structural failure modes of the Church dome.

#### ***Local Buckling***

Thin shell structures are vulnerable to local buckling though it is more typical in constructions of larger spans. Assuming a Young's Modulus,  $E$ , of 300 ksi the critical stress in the tile is 571 psi. The highest calculated internal stress, meridional or hoop, occurs at the base of the dome where  $P_\phi = -53.4$  kips and is equal to 231 psi. With a factor of safety of 2.5, the structure does

not appear to be in danger of local buckling even with this conservative dome thickness. However, local buckling may occur if the dome thickness was reduced in half to 1.21 inches. Using the same assumptions and conservative thickness, the critical distributed load applied is 626 psf, or 1.4 times the highest calculated applied load which occurs at  $\Phi = 70^\circ$ .

### *Cracking and Collapse*

The second limit state examines failure by tension or splaying at the dome base in the case that the metal tension bands are non-existent, are installed improperly, or have experienced extreme loss of section, and that the cylinder wall cannot support this added load. Case Studies 2 and 4 of the graphical approach assume the condition of zero tension capability. Where the compression hoop forces decrease from maximum compression to zero at  $\Phi = 67^\circ$ , thrust line analysis is applied. The thrust line is no longer constrained to the established membrane plane along the centerline of the dome thickness. Instead, its path is determined by the loads applied at the centroids of the remaining dome components and the weight of the vertical cylinder wall below the dome. If the thrust line remains within the assumed thickness of the masonry, then the Church dome will support itself and its applied loads without external tensile reinforcement.

Though difficult to discern due to the scale of the figure, the applied loads on the dome alone do not constrain the free 'tail' of the thrust line from escaping the dome thickness (Appendix C.2). Therefore, if the structural thickness is only 3 in. as assumed in this analysis, the bottom edge of the dome would crack and splay if metal tension bands were not provided. If the effective thickness increases to 8 inches at the base of the dome where  $\Phi$  exceeds  $80^\circ$ , then the line of thrust remains within the dome and transitions into the support structure without the need for tension components in the dome (Appendix C.5). The increased thickness may come from the solid masonry infill at the dome base. Increasing the surcharge at the voussoir 7 (bottom edge of the dome) by 10,000 lbs per lune also shifts the line of thrust back into the effective dome thickness of 3 in.; it must be checked that this increase does not result in local buckling, and it does not (Appendix C.6). In these alternative scenarios, the cylinder wall itself must have tension capabilities to constrain the force line within the structure once the force line travels below the dome extents.

## **Summary**

### ***State of the Art***

In the years preceding the advent of Guastavino construction in America, significant dome construction generally appeared limited to State Capitol buildings and some educational institutions (Melargano, 1991). These domes were typically of heavy masonry construction or cast iron, requiring metal framework to support the dome itself. The introduction of masonry tile vaulting by Guastavino assisted in transforming domes into a more economically viable structure in terms of construction time and materials. Thus in the years between 1900 and World War II, the Guastavino Company played a significant role in proliferating dome construction in other building types such as commercial and religious institutions. In the field of architecture, the Guastavino Company opened possibilities to architects and builders by achieving structural feats once considered impossible and inventing building technologies found in structures across the United States.

### ***The First Church of Christ, Scientist, Dome***

Based on the assumptions and conditions stated in this analysis, the Church dome is indeed capable of carrying its self-weight and applied loads. Guastavino appropriately incorporated tension components, including metal bands and masonry infill, at locations of zero hoop forces where the dome must rely on external means to resist thrust. Without the existing metal tension bands, the dome may experience cracking near its base where the line of thrust travels outside the structure's thickness depending on whether the solid masonry infill at the base is considered part of the structure. In addition to the dome, the Church showcases the beauty and capabilities of Guastavino design and construction, and merits recognition beyond its relative obscurity today.

### ***The End of an Era***

The rising cost of manual labor combined with the increasing presence of thin shell concrete structures in the late 1930s gradually ousted the use of masonry in large scale construction projects. The number of projects involving the Guastavino Company went from nearly thirty to sixty annually between 1905 and 1930 to a trickle of buildings after World War II (Tarragó, 2002). The 1950s saw the completion of the last Guastavino dome, the National Shrine of Immaculate Conception in Washington, D.C. In 1962, 21 years after Guastavino, Jr., sold his remaining shares in the company, the Guastavino Company was liquidated, and the era of thin-tile vaulting in the United States ended.

### ***Future Work***

Numerous aspects of the First Church of Christ, Scientist, and Guastavino construction remain open to further exploration and research. The main auditorium dome contains a number of possibilities, including structural analyses assuming different structural thickness and varying locations of the line of thrust in both the meridional and hoop direction. The Church houses a number of other works by Guastavino, such as the shallow basement dome built in the first phase of construction, any of which will provide fascinating insight into Guastavino's design rationale. Finally, a study of other Guastavino dome projects from the earlier to the later years will provide knowledge of the evolution of Guastavino's mastery of structural design. Such a study may focus on domes such as the Cathedral of St. John the Divine and the Benjamin Franklin Memorial in Philadelphia, built a couple years after the First Church of Christ, Scientist, with a similar design.

## Figures

*In order of citation in text.*



Figure 1. The first phase of construction terminated at the belt course (First Church, 1996).

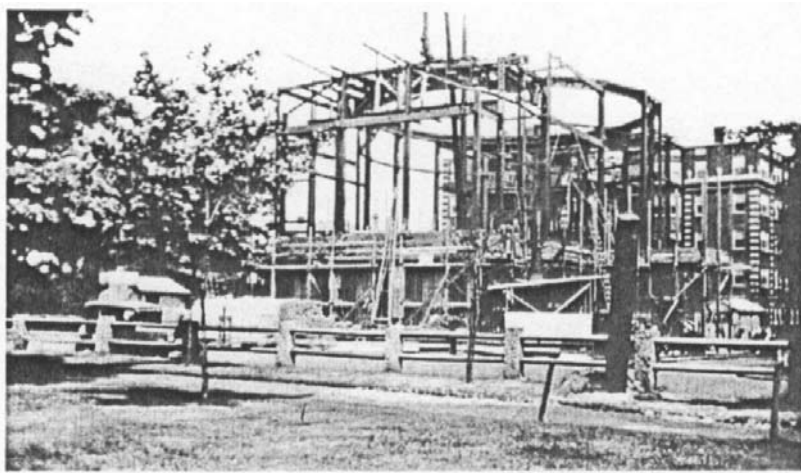


Figure 2. Second phase of construction: the steel circular base support for the auditorium dome (First Church, 1996).



Figure 3. The church held its first services on 30 April 1930, and dedicated the building on 23 May, 1937 (First Church, 1996).



Figure 4. Strength test of a 12 ft span timbrel vault, three courses thick, supporting a load of 112,578 lbs of pig iron (23 May 1901) (Tarragó, 2002).

**SOME DOMES CONSTRUCTED BY  
R. GUASTAVINO CO.**

BOSTON		NEW YORK			
BUILDING and LOCATION	SPAN	ARCHITECTS	BUILDING and LOCATION	SPAN	ARCHITECTS
1. Cathedral, St. John the Divine, New York City	110 ft.	Heine & La Farge	6. University of New York, New York City	100 ft.	McKim, Mead & White
2. National Museum, Washington, D. C.	80	Huntress & Marshall	7. McKinley National Memorial, Canton, Ohio	50	H. Van Hook, Montgomery Hawley & Nickerson
3. Institute of Arts and Sciences, Brooklyn, N. Y.	44	McKim, Mead & White	8. St. Paul's Chapel, Columbia U., N. Y. City	32	
4. St. Francis de Sales Church, Philadelphia, Pa.	42	Henry D. Dapp	9. Knoll Shores Synagogue, Pittsburgh, Pa.	28	Palmer & Hueston
5. Bank of Montreal, Montreal, P. Q.	40	McKim, Mead & White and A. T. Taylor	10. University of Virginia, Charlottesville, Va.	25	McKim, Mead & White
6. Church of St. Barbara, Brooklyn, N. Y.	42	McKim, Mead & White	11. Elgin Hotel, Boston Park, New York City	24	Heine & La Farge
7. General Trust Company, Philadelphia, Pa.	102	McKim, Mead & White and Allen Smith	12. Madison Sq. Postal & Clerical, N. Y. City	40	McKim, Mead & White
			13. J. J. Jones Memorial Library, Sag Harbor, N. Y.	30	Augustus N. Adams

Figure 5. Select timbrel domes designed by the Guastavino Company, many of which preceded Guastavino, Sr., death (Avery Library, Columbia University).



Figure 6. Interior of the main dome.

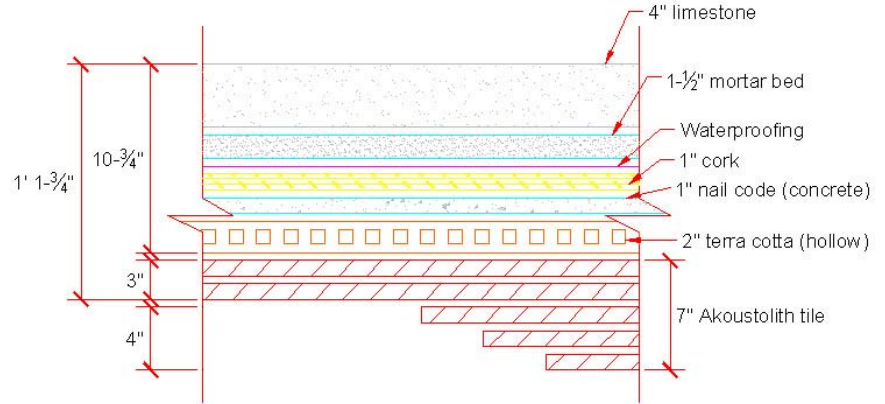


Figure 7. Typical section through main dome.

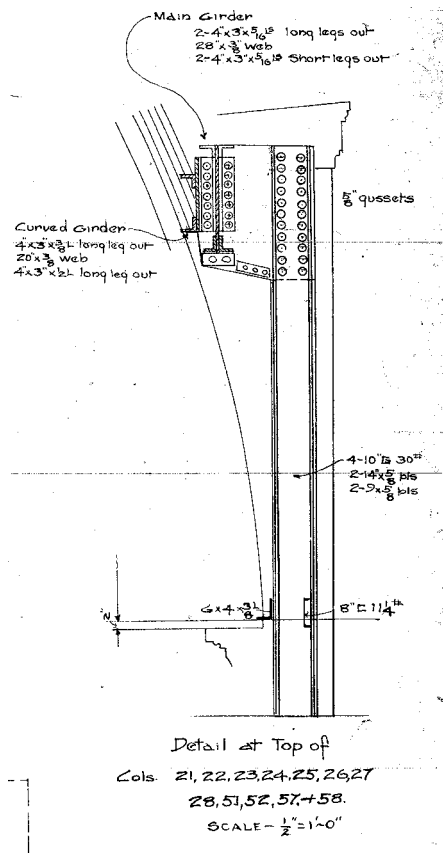


Figure 8. Section detail of metal reinforcement at dome base and top of support wall (Shedd, 1922).

THIS IS ALSO IN  
SWEETS  
1942  
1941

## AKOUSTOLITH SOUND-ABSORBING STONE

**SIZES AND SHAPES AS DESIRED**

- A PERMANENT, MASONRY MATERIAL
- INCOMBUSTIBLE
- INTEGRAL COLORS AND TEXTURES AS REQUIRED
- SOUND ABSORPTION UP TO 95% AT C.

The illustration shows AKOUSTOLITH cast into large coffers and used as the soffit course of a structural GUASTAVINO dome more than 80 feet in diameter.

*See our catalog in Sweets'*

FRANKLIN HALL  
BENJAMIN FRANKLIN MEMORIAL  
PHILADELPHIA, PA.  
JOHN T. WINDRIM, ARCHITECT

**R. GUASTAVINO COMPANY**  
500 FIFTH AVE., NEW YORK    40 COURT ST., BOSTON

*Reprinted from the April, 1940, issue of ARCHITECTURAL RECORD*

Figure 9. Akoustolith tile advertisement (Avery Library, Columbia University).



Figure 10. Corrugated surface of the structural and hollow terra cotta tiles.



Figure 11. Installation of coffers in dome structure at the Benjamin Franklin Memorial, Philadelphia (1933) (Avery Library, Columbia University).

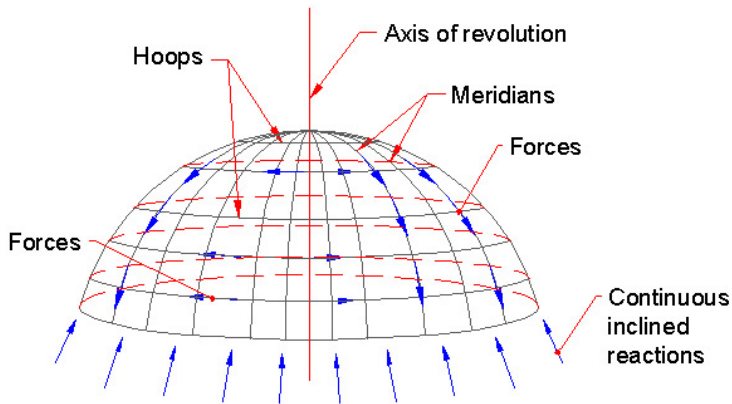


Figure 12. Summary of dome behavior.

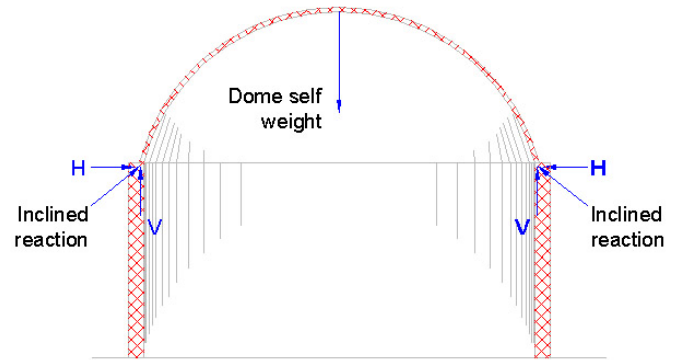


Figure 13. Horizontal and vertical components of the inclined reaction at the dome base and support structure.

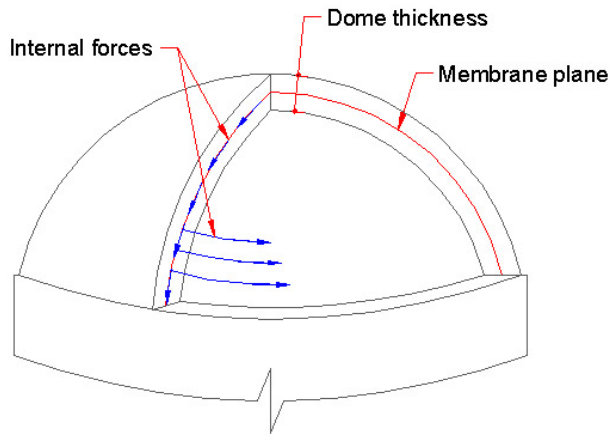


Figure 14. The membrane plane is assumed at the centerline of the dome thickness.

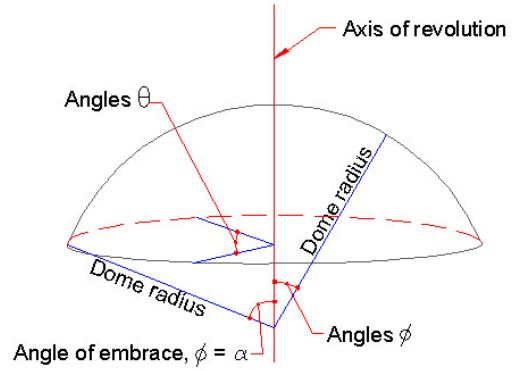


Figure 15. Dome parameters and terms.

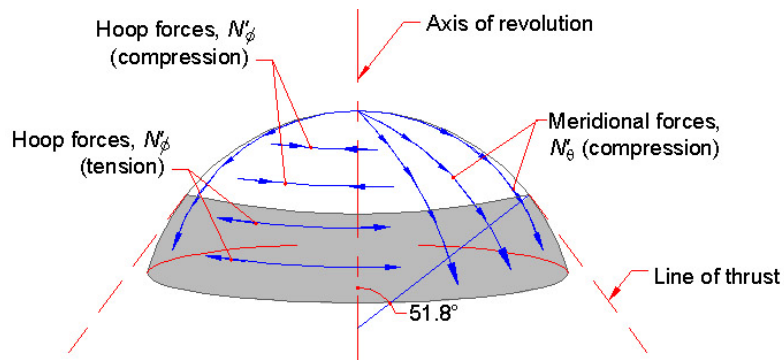


Figure 16. Direction of internal meridional and hoop forces for a uniformly loaded axisymmetrical dome.

Figure 17. Dome Geometry		
Parameter	Symbol	Value
Dome radius (ft)	$a$	32.8
Dome thickness (ft)	$t$	0.25
Skylight radius (ft)	$r_i$	6.0
Dome surface area (ft <sup>2</sup> )		6171
Horizontal projection (ft <sup>2</sup> )		3387
Thickness to radius ratio		0.008
Angle of enclosure (deg.)	$\alpha$	85.9
Location of steel girder (deg.)	$\Phi_g$	71.5
Location of tension band (deg.)	$\Phi_t$	54.9
Location of skylight edge (deg.)	$\Phi_i$	10.5

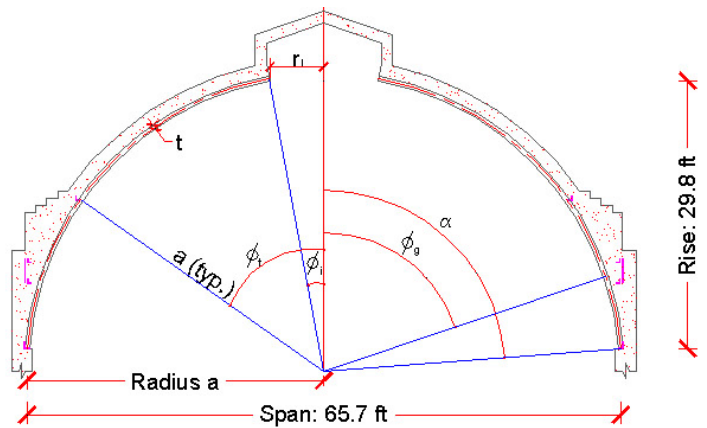


Figure 17. Parameters for the main auditorium dome of the First Church of Christ, Scientist, Cambridge.

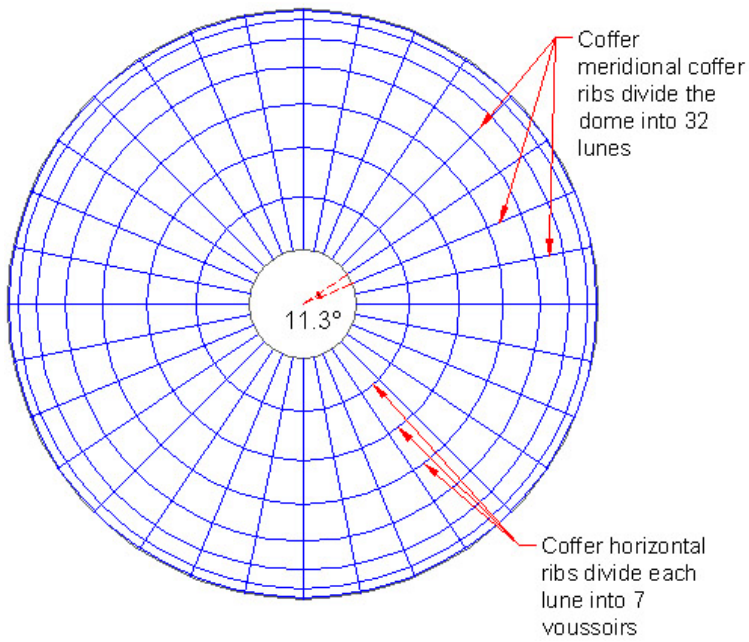


Figure 18. Coffe ribs divide the main dome into lunes and voussoirs (plan view).

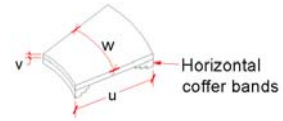


Figure 19. Dimension parameters for a typical voussoir.

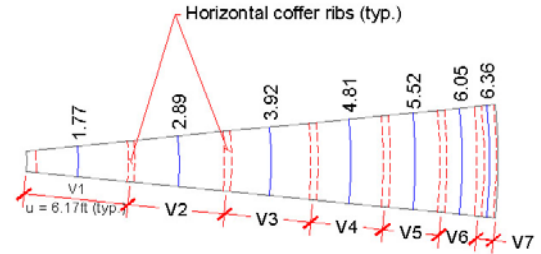


Figure 20. Average width,  $w$ , of each voussoir in a typical lune (ft). Plan view.

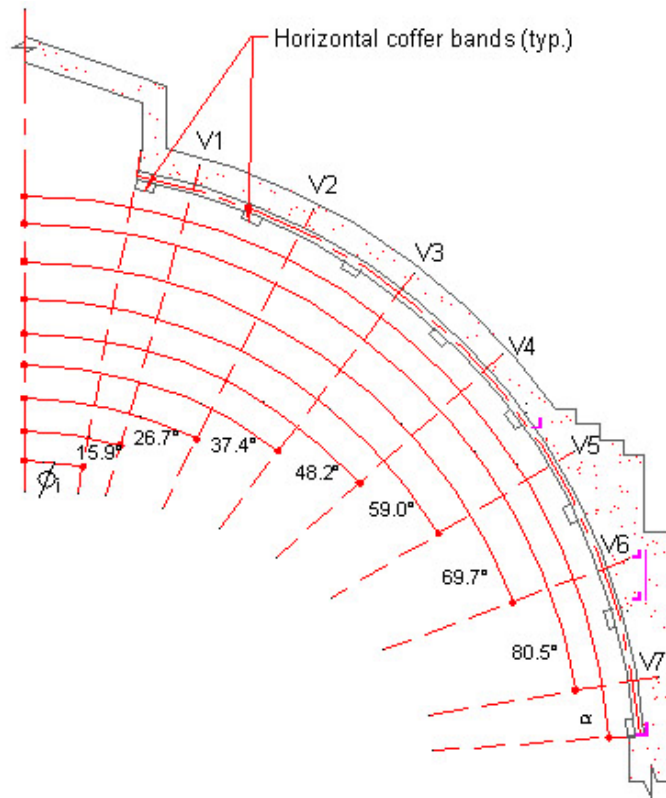


Figure 21. Values of angle  $\Phi$  defining each voussoir along a lune.

Material	Applied Load		
	psf	lbs/ft	kips
Overburden (roof cladding)	95.2		
Akoustolith Tiles	14.0		
Underburden (tile bands/ridges)	14.2		
Uniform Dead Load, $w_d$	123.4		
Uniform Live Load, $w_l$	22.0		
<b>Total Uniform Load, <math>w_u</math></b>	<b>145.4</b>		<b>897</b>
<b>Skylight Line Load, <math>p</math></b>		<b>117</b>	<b>4.40</b>
<b>Variable Surcharge, <math>q'</math></b>	<b>475</b>	<b>4170</b>	<b>803</b>
<b>Total Weight of Dome, <math>W</math></b>			<b>1705</b>

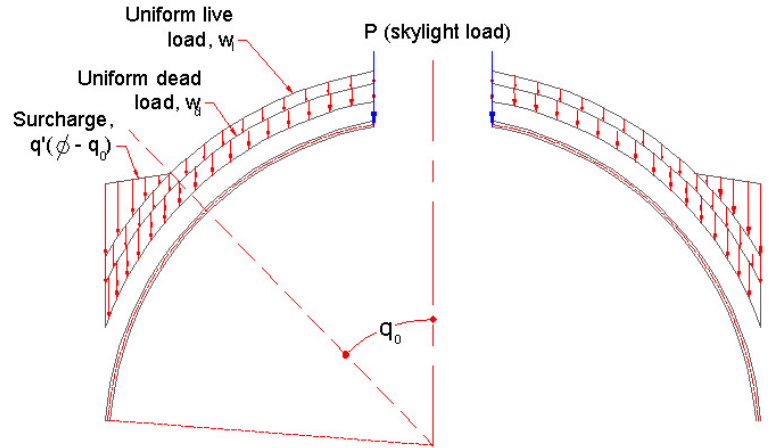


Figure 22. Magnitude and location of applied loads.

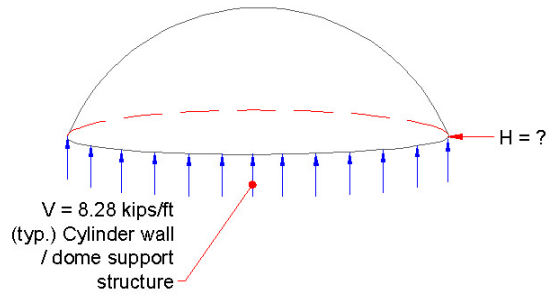


Figure 23. Vertical reaction at the base of the dome.

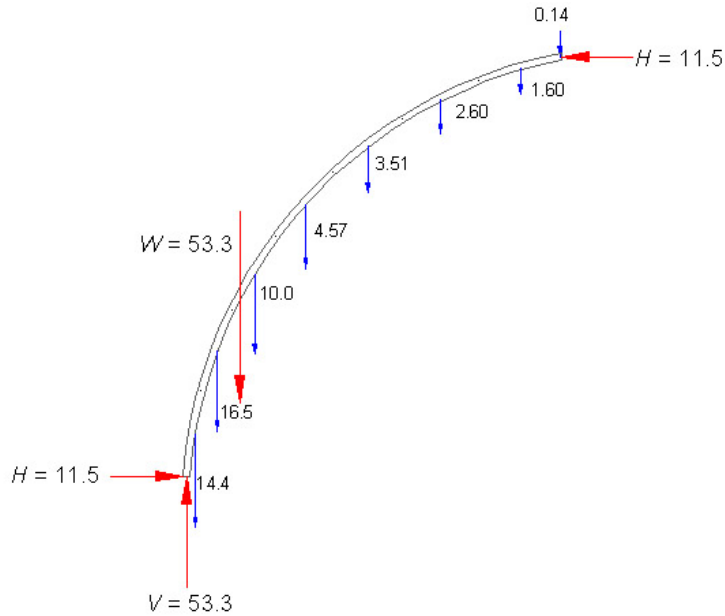


Figure 24. Summary of applied forces and reactions on the dome (kips).

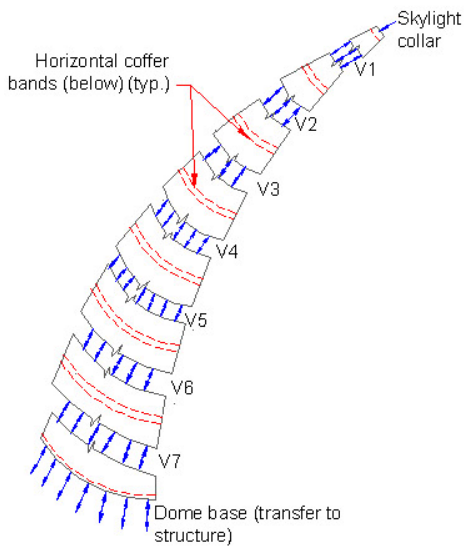


Figure 25. Schematic representation of meridional force locations for a typical lune

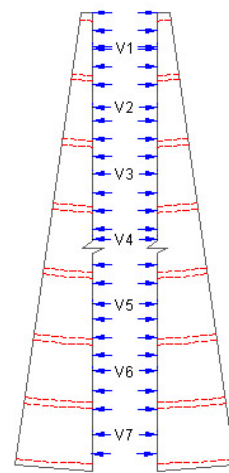


Figure 26. Schematic representation of hoop force locations for a typical lune

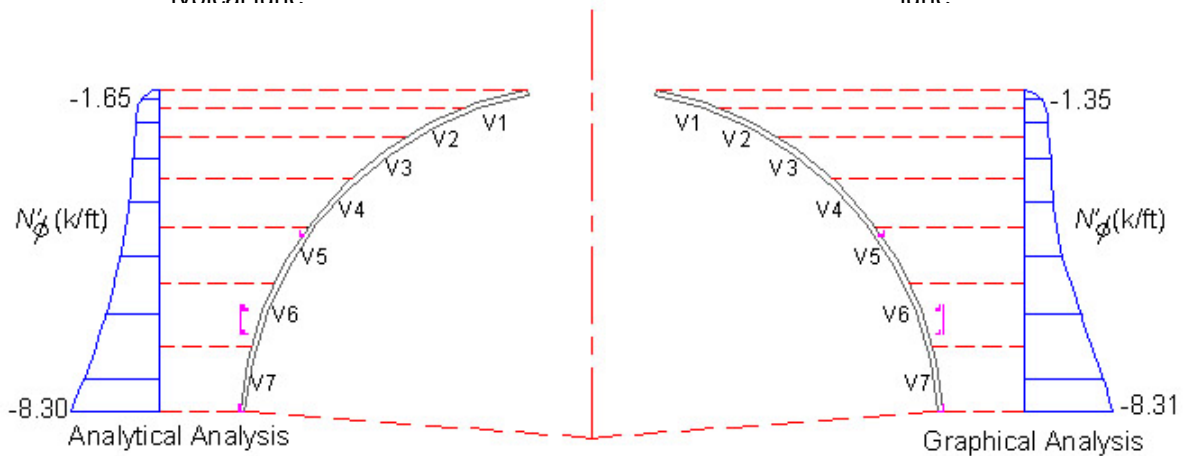


Figure 27. Comparison of meridional stress resultants from crown to base from analytical and graphical methodologies (negative values indicate compression).

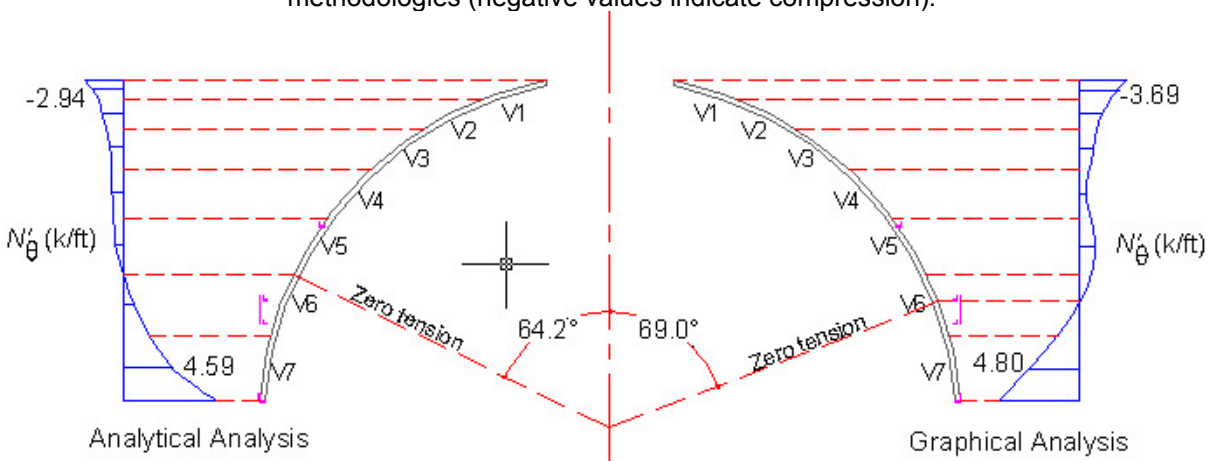


Figure 28. Comparison of hoop stress resultants from crown to base from analytical and graphical methodologies (negative values indicate compression). Note the effect of surcharge on the location of zero hoop forces.

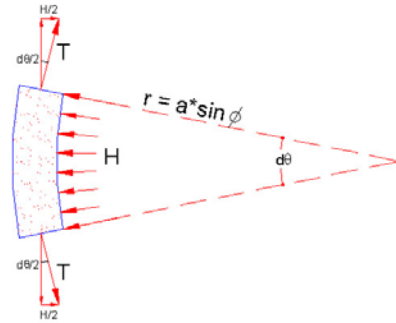


Figure 29. Tension hoop forces,  $T$ , compensate for the thrust,  $H$ , generated by the meridional forces.

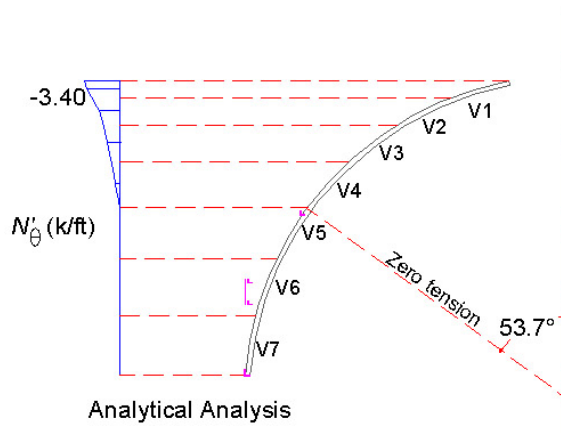


Figure 30. Hoop stress resultant before installations of stone cornices and skylight. Note the location of the uppermost tension band with the zero tension line.

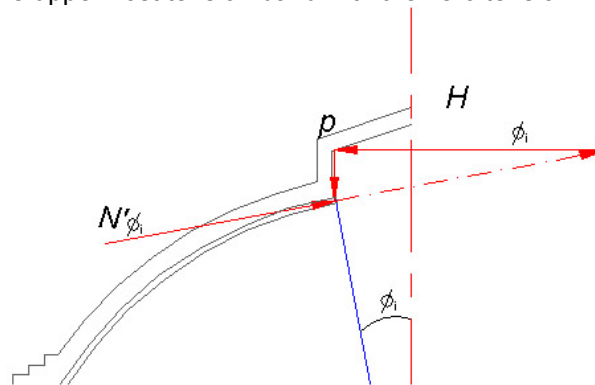


Figure 31. Forces generated by the line load,  $p$ , must be resisted with a compression ring.

## Tables

In order of citation in text.

Table 1. Graphical Structural Analysis Conditions for Each Case Study.

Case Study	Load Condition	Structural Tensile Capacity
1	Variable	Yes
2	Variable	No
3	Uniform	Yes
4	Uniform	No

Table 2. Internal Force Equations for the Membrane Analysis.

	Description	Notation	Formula
Meridional Stress Resultants (force per length)	For spherical domes with a uniform load at any angle $\Phi$	$N'_\phi$	$-aq\left(\frac{1}{1+\cos\phi}\right)$
	For spherical domes with a concentrated load, $P$ , at the axis of revolution	$N''_\phi$	$-\frac{P_c}{2\pi a \sin^2\phi}$
	For spherical domes with variable load, $q'$ , that increases for angle $\Phi < \Phi_0$	$N'''_\phi$	$-\left(\frac{aq'}{\sin^2\phi}\right)\left[\sin\phi - \sin\phi_0 - (\phi - \phi_0)\cos\phi\right]$
Hoop Stress Resultants (force per length)	For spherical domes with a uniform load at any angle $\theta$	$N'_\theta$	$aq\left(\frac{1}{1+\cos\phi} - \cos\phi\right)$
	For spherical domes with a concentrated load, $P$ , at the axis of revolution	$N''_\theta$	$\frac{P_c}{2\pi a \sin^2\phi}$
	For spherical domes with a variable load, $q'$ , that increases for angle $\Phi < \Phi_0$	$N'''_\theta$	$-\frac{aq'}{\sin^2\phi}\left[2(\phi - \phi_0)\cos\phi - (\phi - \phi_0)\cos^3\phi - \sin\phi + \sin\phi_0\right]$

Table 3. Comparison of Meridional Force Values for Case Study 1.

Voussoir	$\Phi$ (degrees)	Analytical Analysis		Graphical		Percent Difference
		$N_{total\Phi}$ (kips/ft)	Meridional Load (kips)	$N_{total\Phi}$ (kips/ft)	Meridional Load (kips)	
1	15.9	-1.65	-2.91	-1.35	-2.39	17.9%
2	26.7	-2.23	-6.45	-2.24	-6.49	0.7%
3	37.4	-2.50	-9.80	-2.53	-9.90	1.0%
4	48.2	-2.81	-13.5	-2.72	-13.1	3.1%
5	59.0	-3.65	-20.2	-3.58	-19.8	1.8%
6	69.7	-5.03	-30.4	-5.40	-32.7	7.5%
7	80.5	-7.01	-44.6	-7.39	-47.0	5.3%
Base, alpha	85.9	-8.30	-53.4	-8.31	-53.4	0.1%

Table 4. Comparison of Hoop Force Values for Case Study 1.

Voussoir	$\Phi$ (degrees)	Analytical Analysis		Graphical Analysis		Percent Difference
		$N_{total\theta}$ (kips/ft)	Hoop Load (kips)	$N_{total\theta}$ (kips/ft)	Hoop Load (kips)	
1	15.9	-2.94	-18.2	-3.69	-22.8	25%
2	26.7	-2.04	-12.6	-2.08	-12.8	2.1%
3	37.4	-1.29	-7.95	-1.30	-8.00	0.5%
4	48.2	-1.12	-6.93	-0.62	-3.81	45%
5	59.0	-0.90	-5.58	-1.41	-8.71	56%
6	69.7	0.95	5.86	0.18	1.12	81%
7	80.5	4.59	28.3	4.80	29.6	4.7%

Table 5. Horizontal Thrust from the Analytical Approach for Case Study 1.

Voussoir	$\Phi$ (degrees)	Horizontal Thrust Outward (kips)
Skylight collar	10.5	0.00
1	15.9	2.80
2	26.7	5.76
3	37.4	7.78
4	48.2	9.01
Tension band	54.9	
5	59.0	10.40
6	69.7	10.54
Tension band at girder	71.5	
7	80.5	7.38

## References

- American Institute of Steel Construction (1998). *Manual of Steel Construction – Load & Resistance Factor Design: Volume 1*. 2<sup>nd</sup> ed. Chicago: AISC.
- Bigelow, H. F., & Wadsworth, P. (1922 – 1929). *First Church of Christ, Scientist, Cambridge, Massachusetts*. [Blueprint design drawings]. Boston: Bigelow and Wadsworth, Architects.
- Billington, D. P. (1982). *Thin Shell Concrete Structures*. New York: McGraw-Hill Book Co.
- Cambridge Historical Commission. (1973). *Survey of Architectural History in Cambridge, Report 4: Old Cambridge*. Cambridge, MA: The Cambridge Historical Commission.
- City of Cambridge, Massachusetts (1924). *Zoning Law and Building Code 1924*. Cambridge, MA: City of Cambridge.
- First Church of Christ, Scientist. (1996). *History of the First Church of Christ, Scientist, Cambridge, 1899 – 1996*. Cambridge, MA: First Church of Christ, Scientist.
- Guastavino, R. (1929). *Drawing No. 9 - Dome Section: First Church of Christ, Scientist, Cambridge, Massachusetts*. [Blueprint drawing]. New York: R. Guastavino Co.
- Guastavino, R. (1893). *Essay on the Theory and History of Cohesive Construction, Applied Especially to the Timbrel Vault*. Boston: Ticknor and Company.
- Heyman, J. (1977). *Equilibrium of Shell Structures*. Oxford: Clarendon Press.
- Heyman, J. (1995). *The Stone Skeleton*. Cambridge: Cambridge University Press.
- Heyman, J. (1996). *Arches, Vaults and Buttress*. Hampshire, Great Britain: Variorum.
- Huerta, S. (2003). The Mechanics of Timbrel Vaults: A Historical Outline. In A. Becchi (ed.) *Essays on the History of Mechanics* (pp. 89-133). Boston: Birkhauser Verlag.
- Huerta, S., López, G., & Redondo, E. (1999). *Las bóvedas de Guastavino en América*. Madrid: Instituto Juan de Herrera.
- Massachusetts Committee for the Preservation of Architectural Records (COPAR). (1984). *Directory of Boston Architects, 1846-1970*. Cambridge: COPAR.
- Melargano, M. (1991). *An Introduction to Shell Structures: The Art and Science of Vaulting*. New York: Van Nostrand Reinhold.
- Parks, J. (1996). *The Old World Builds the New: The Guastavino Company and the Technology of the Catalan Vault (1885-1962)*. New York: Avery Architectural and Fine Arts Library.
- Pounds, R., Raichel, D., & Weaver, M. (1999). The Unseen World of Guastavino Acoustical Tile Construction: History, Development, Production. *APT Bulletin*, 30(4), pp. 33-40.

- Shedd, C. L. (1922). *First Church of Christ, Scientist, Cambridge, Massachusetts*. [Blueprint structural drawings]. Boston: Bigelow and Wadsworth, Architects.
- Tarragó, S. (2002). *Guastavino Co. Catalogue of Works in Catalonia and America (1885-1962)*. Barcelona: Col.legi d'Arquitectes de Catalunya.
- Wolfe, W. S. (1921). *Graphical Analysis: A textbook on graphic statics*. New York: McGraw-Hill Book Co.

## **Appendices**

### **A. Select Project Drawings**

1. Original blueprints by Bigelow and Wadsworth (1922 – 1929).
  - a. *Drawing 9 – Front Elevation*
  - b. *Drawing 13 – Longitudinal Section*
  - c. *Drawing 8 – Roof Plan*
  - d. *Drawing 23 – Roofing Plan (Structural)*
2. *Drawing No. 9 - Dome Section: First Church of Christ, Scientist, Cambridge, Massachusetts*, by R. Guastavino Co.

### **B. Supplementary Documents**

1. Excerpts from the Cambridge, MA, newspaper, *The Cambridge Tribune*.
  - a. (12 Jan 1924). "Corner Stone of Church Edifice is Laid at Early Dawn."
  - b. (13 Sep 1924). "Sunday Services in Christian Science Sunday School Room."
  - c. (18 May 1924). "First Church of Christ Scientist to Be Completed."
  - d. (12 April 1930). "Christian Science Church Auditorium is Now Completed." (2 pp).
2. Construction Correspondence
  - a. (24 Aug 1920 and 2 March 1922). Internal - R. Guastavino Co. cover letter and initial cost estimates
  - b. (4 Apr 1922) R. Guastavino Co. and J. G. White Eng. Corp.
  - c. (18 Feb 1929) R. Guastavino Co. and L.D. Willcutt & Sons Co.
  - d. (1 May 1929) L.D. Willcutt & Sons Co. and R. Guastavino Co.
  - e. (31 Dec 1929) R. Guastavino Co. expense sheet
  - f. (12 Nov 1931) Wadsworth, Hubbard & Smith and R. Guastavino Co.
3. United States Patent 947,177 Masonry Structure (18 Jan. 1910)
4. Guastavino Archive Collections from Avery Library, Columbia University
  - a. Sweet's Catalog advertisement for R. Guastavino Company (1944?)
  - b. Compressive test results (May 1927 and February 1935)
  - c. List of known stress diagrams for Guastavino buildings.

### **C. Graphical Analyses**

1. Case Study 1
2. Case Study 2
3. Case Study 3
4. Case Study 4
5. Case Study 2 with increased thickness
6. Case Study 2 with increased surcharge at dome base

### **D. Analytical Analyses**

1. Parameters
2. Loads
3. Case Study 1
4. Case Study 3

### **E. Notes and Calculations**